DOI 10.5012/bkcs.2010.31.12.3675

In Situ X-ray Absorption Spectroscopic Study for α-MoO_3 Electrode upon Discharge/Charge Reaction in Lithium Secondary Batteries

Joo-Hee Kang, Seung-Min Paek,†,* and Jin-Ho Choy*

*Center for Intelligent Nano-Bio Materials (CIMBN), Department of Chemistry and Nanoscience, and Department of Bioinspired Science, Ewha Womans University, Seoul 120-750, Korea. *E-mail: jhchoy@ewha.ac.kr*
*†Department of Chemistry, Kyungpook National University, Taegu 702-701, Korea. *E-mail: smpaek@knu.ac.kr*
Received August 21, 2010, Accepted October 9, 2010

In-situ X-ray absorption spectroscopy (XAS) was used to elucidate the structural variation of α-MoO_3 electrode upon discharge/charge reaction in a lithium ion battery. According to the XAS analysis, hexavalent Mo atoms in α-MoO_3 framework are reduced as the amount of intercalated lithium ions increases. As lithium de-intercalation proceeds, most of pre-edge peaks are restored again. However, according to the Fourier transforms of the extended X-ray absorption fine structure (EXAFS) spectra, lithium de-intercalation reaction is partially irreversible upon the charge reaction, which is one of the main reasons why the capacity of α-MoO_3 electrode decreases upon successive discharge/charge cycles.

Key Words: X-ray absorption spectroscopy, Layered material, Lithium secondary battery

Introduction

MoO_3 has been extensively investigated as a key material for not only fundamental research but also technological applications in optical devices, smart windows, catalysts, sensors, lubricants, and electrochemical energy storage.[1-5] Within its many distinctive properties, two-dimensional layered structure of *orthorhombic* MoO_3 (α-MoO_3) presents open channels for rich intercalation chemistry, especially for the potential application as lithium secondary batteries.[6]

In rechargeable Li ion batteries (LIB), Li ions can be intercalated and de-intercalated from the host materials during charge/discharge reaction. A good electrode should have high reversibility toward Li intercalation/de-intercalation. Because such a reversibility of an electrode is deeply correlated with the structural variation upon charge/discharge reaction, it is quite important to investigate the relationship between a local structure and an electrochemical property during cycling in LIB. Since X-ray absorption spectroscopy (XAS) is a powerful tool to probe the electronic and local structure of electrodes, XAS can be effectively used for the local structural refinement during electrochemical reaction of electrodes in LIB.[7] For example, an oxidation state of an active material in an electrode can be quantitatively determined by X-ray absorption near edge structure (XANES) analysis, and structural parameters such as interatomic distances, coordination numbers, and Debye-Waller factors can be also explored by the extended X-ray absorption fine structure (EXAFS).

In this study, the structural investigation on α-MoO_3 electrode has been carried out by *in situ* XAS. The layered MoO_3 has very large discharge capacity, which makes this compound attractive as an electrode in LIB. However, the reversibility of α-MoO_3 is not so good upon the successive cycling.[8] The reason for poor cyclability will be discussed, based on the structural information obtained by *in situ* XAS experiments.

Experimental Section

The layered molybdenum oxide (α-MoO_3, Aldrich) was heat-treated at 250 °C for 1 h to remove moisture on the surface, and ground to fine powder. According to the scanning electron microscope (SEM) image, the particle size of α-MoO_3 is in the range around several micrometers (Supplementary Materials). Electrochemical measurements were performed using a pouch-type cell with the aid of a computer-controlled potentiostat/galvanostat system. The pouch-type cell for charge/discharge was constructed, in which the electrode was made by intimately mixing 70% MoO_3, 25% Ketjenblack, and 5% poly(tetrafluoroethylene). This electrode was dried under vacuum at 80 °C for 3 h, and introduced into an argon-filled glovebox without any exposure to air. The electrolyte was 1M $LiPF_6$ in a 1:1 (v/v) mixture of ethylene carbonate and dimethyl carbonate, and a lithium foil was used as a reference electrode and anode, respectively. For discharge/charge experiments, a constant current was applied between 1.4 and 4.3 V (*vs* Li^+/Li) with a current density of 10 mA/g.

XAS experiments at the Mo K-edge were performed with the X-ray absorption fine structure (XAFS) facility installed at beamline 7C in Pohang Accelerator Laboratory (PAL), Korea. *In situ* XAS data were collected at room temperature in a transmission mode, during which a constant current density of 10 mA/g was used for charge/discharge with a potential window between 1.4 and 4.3 V. All the present spectra were calibrated by measuring the spectra of Mo metal foil simultaneously with those of the samples. A Si(111) double crystal monochromator (DCM) was employed to monochromatize the X-ray photon energy. A step size was 0.2 eV in the XANES region in order to accurately collect the XANES spectra. Data analysis using UWXAFS 2.0 code was carried out by the standard procedure as reported previously.[9,10] Briefly, the inherent background was removed by fitting a polynomial to the pre-edge region and

extrapolating it over the entire spectrum. The resulting EXAFS spectra after background removal and normalization were k^3-weignted, and then, Fourier-transformed in the range from 2.9 to 13.2 $Å^{-1}$.

Results and Discussion

Figure 1(a) shows the crystal structure of layered MoO_3 that is used for electrode in this study. In α-MoO_3, [MoO_6] octahedra share their edges along the *a*-direction and are interlinked with their corners along the *c*-direction to form a sheet in the *ac*-plane. The weak van der Waals interactions along the *b*-direction allow Li ions to be intercalated between layers. On the other hand, the charge/discharge curves of MoO_3 are shown in Figure 1(b). The discharge curve (Li intercalation) exhibits two plateaus, the first one at about 2.8 V and the second one at the potential range from 2.4 to 2.0 V. According to the previous report on the *in situ* XRD analysis, the first plateau is related with an increase of van der Waals gap along the crystallographic *b*-direction, which is due to the intercalation of solvated Li ions.[11] The second plateau can be indexed to the further intercalation of Li ions, which induces further distortion of [MoO_6] octahedra.

To probe the structural variation upon discharge/charge, *in situ* Mo K-edge XANES analysis during the first discharge/charge cycle was conducted. The layered MoO_3 shows a pre-edge feature around 20000 eV, which is assigned as the transition from the core 1*s* level to the unoccupied 4*d* state.[12,13] The existence of pre-edge peak is related with the local symmetry around Mo atoms. In the starting layered MoO_3, distortion from an ideal octahedral symmetry removes the inversion center and induces hybridization between *p* and *d* orbitals, leading to the well-distinct pre-edge peak. As the amount of the intercalated Li ions increases upon discharge, the pre-edge peak disappears and the main absorption edge shifts to the lower energy.

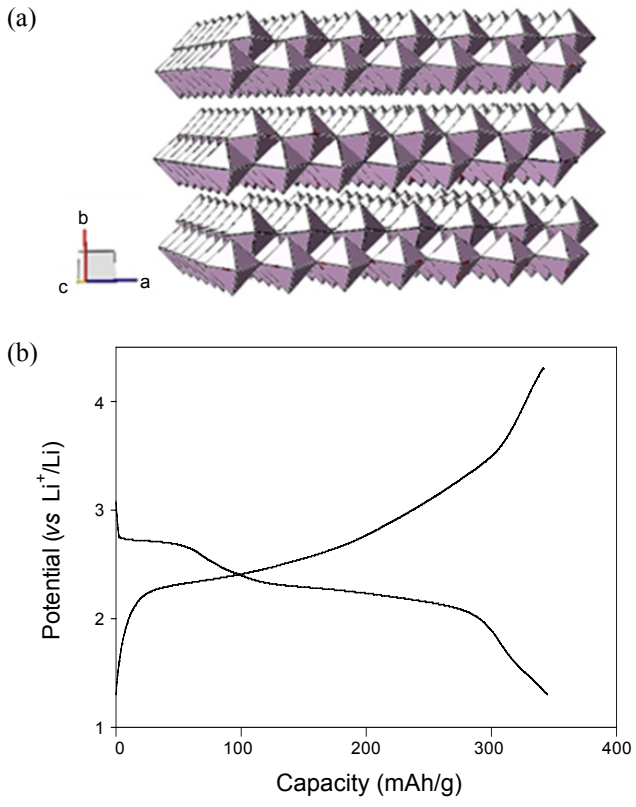

Figure 1. (a) The crystal structure of layered MoO_3. (b) charge/discharge curves for layered MoO_3 during the first cycle.

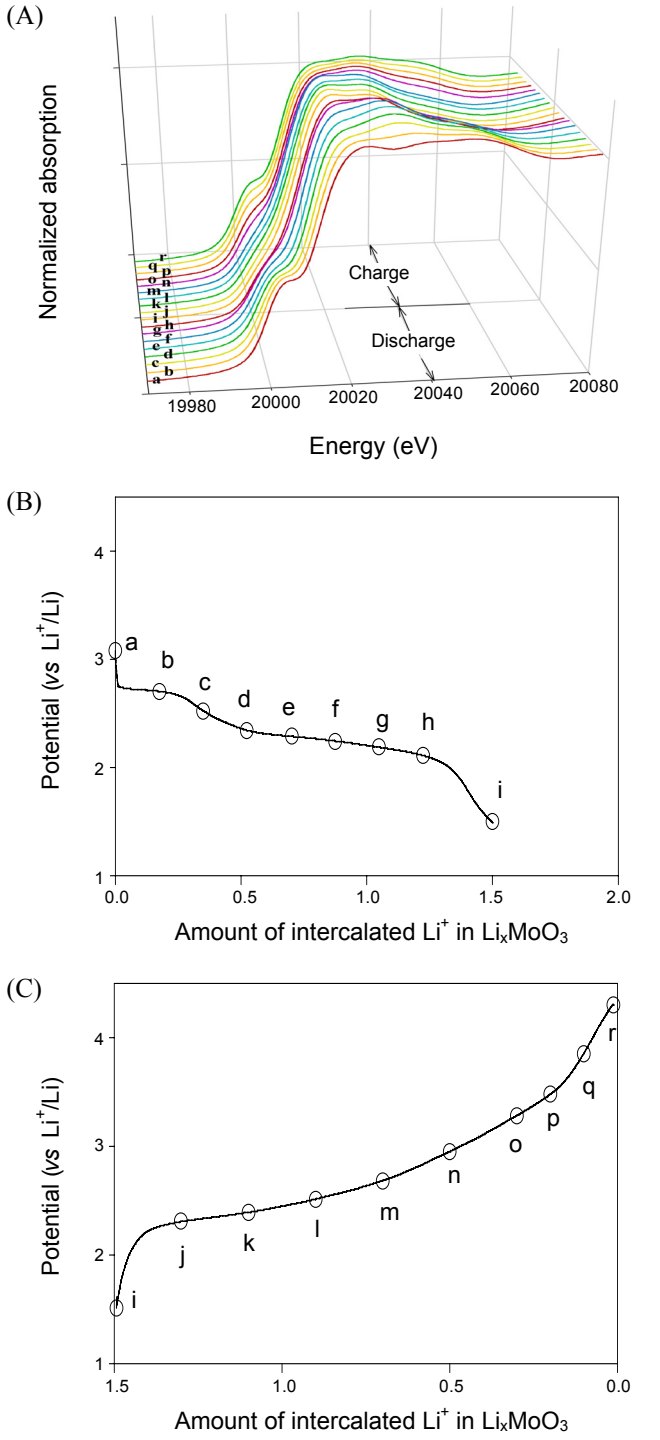

Figure 2. (A) *In situ* Mo K-edge XANES spectra for α-MoO_3 during the first discharge/charge cycle. (B) The first discharge and (C) charge curves. Each XANES spectrum was obtained at the given point as indicated in discharge/charge curves (from **a** to **r**).

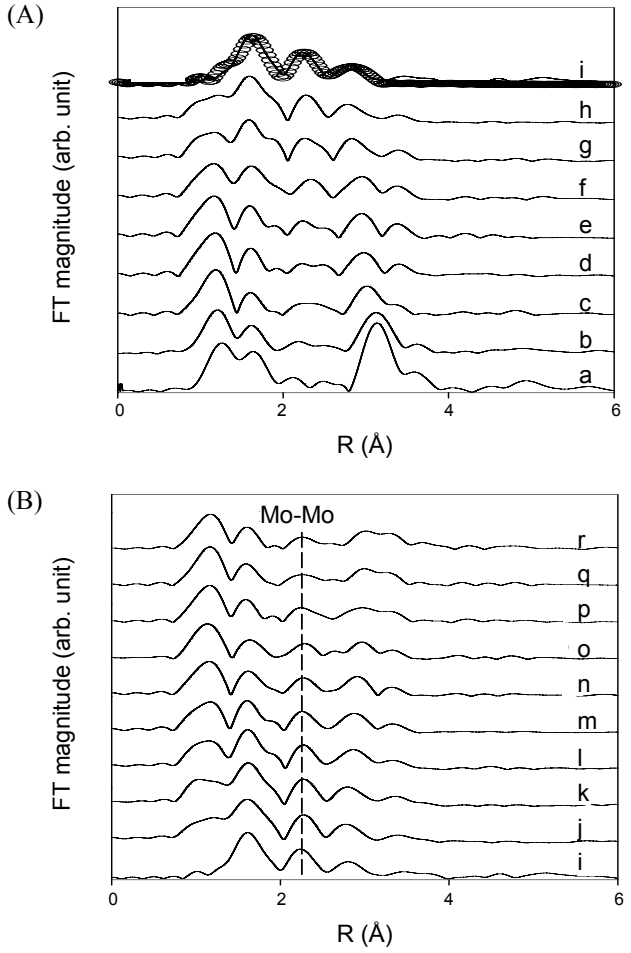

Figure 3. Spectral variation of FT magnitudes for Mo K-edge EXAFS spectra during (A) the discharge and (B) the charge in the first cycle. Each EXAFS spectrum for FT was obtained simultaneously with XANES spectrum. Open circles represent the EXAFS fitting result for spectrum **i**.

Such a change suggests that the average oxidation state of the molybdenum ions in the α-MoO_3 decreases during discharge reaction. Similar results are found in the previous literatures, in which reduced MoO_3 resulted in decreased pre-edge peaks.[14-16] As seen in Figure 2A (from spectrum **a** to **i**), the pre-edge features gradually disappear as the discharge reaction proceeds. The complete disappearance of pre-edge feature after full discharge (Figure 2A, spectrum **i**) clearly shows that hexavalent Mo ions are reduced to the tetravalent and pentavalent ones, suggesting that the α-MoO_3 was transformed into Li_xMoO_3 phase during the galvanostatic discharge reaction. Li/MoO_3 batteries with liquid electrolytes are known to have about 1.5 electrons/mol of MoO_3, corresponding to the composition of $Li_{1.5}MoO_3$ at the fully charge state. On the other hand, as the charge reaction (Li de-intercalation) proceeds, from spectrum **i** to **r**, the characteristic pre-edge peak is gradually restored. Most of characteristic pre-edges are clearly shown especially in the spectra from **p** to **r**. However, according to closer inspection of XANES spectra, an intensity of the pre-edge peak after first cycle (spectrum **r**) is slightly smaller than that of the pristine MoO_3 (spectrum **a**), implying that some of reduced molybdenum ions are not fully oxidized during the first charge process. Such irreversible changes in the oxidation states of molybdenum ions of α-MoO_3 could be one of reasons for the capacity fading in the MoO_3-based LIB.

Table 1. Results of nonlinear Least-Squares curve-fitting analysis for the Mo K-Edge EXAFS spectrum of the fully charge electrode

Compound	Shell	[b]N	[c]R (Å)	[d]σ^2 (Å^2)
[a]Li_2MoO_3 (reference)	Mo-O	6	2.008	
	Mo-Mo	2	2.580	
	Mo	2	3.180	
$Li_{1.5}MoO_3$	Mo-O	6	2.088	0.0074
	Mo-Mo	2	2.628	0.0092
	Mo	2	3.228	0.0122

[a]The crystallographic data for the Li_2MoO_3 was obtained from the reference 17. [b]Coordination numbers. [c]Bond distances. [d]Debye-Waller factors. Errors in σ^2 are 15%, and those in R are 0.02 Å.

The Fourier transforms (FTs) are obtained from the k^3-weighted Mo K-edge EXAFS spectra of MoO_3 during the first discharge/charge reaction (Figure 3A and 3B). In the pristine MoO_3 before electrochemical lithium storage (spectrum **a** in Figure 3A), two FT peaks below 2 Å (non-phase-shift-corrected) can be indexed to Mo-O bonds ranged from 1.67 to 2.34 Å, and the FT peaks from 3 to 4 Å are due to the Mo-Mo neighboring atoms ranged from 3.44 to 3.96 Å. As shown in Figure 3a, the first electrochemical Li uptakes induce considerable structural change. As seen in Figure 3A, two FT peaks from Mo-O bonds are gradually merged into a broad peak during the reduction. The spectrum **i** for the composition of $Li_{1.5}MoO_3$, which is obtained after full discharge, FT spectrum shows only one peak for neighboring oxygen atoms. Such a large structural variation indicates that the first neighboring oxygen atoms ranged from 1.67 to 2.34 Å are rearranged to singlet-like Mo-O shell. Furthermore, the spectrum **i** after the full discharge, shorter Mo-Mo distances at ~2.2 and ~2.8 Å (non-phase-shift-corrected) are observed in the second and third shells of fully discharged electrode, which is due to the considerable rearrangement of molybdenum atoms during charge reaction by the deep Li intercalation. Such shorter Mo-Mo bonds for Li_xMoO_3 could be observed in the reduced lithium molybdenum oxide compounds such as Li_2MoO_3, which has Mo-Mo distances at ~2.6 and ~3.2 Å (phase-shift-corrected).[17]

For the precise determination of bond distances at the fully discharged state, the nonlinear least-squares curve fitting analysis for EXAFS spectrum **i** was conducted in the range $R \leq 3.2$ Å, in which the coordination numbers are fixed. The fitting results are shown in Figure 3A and Table 1. Li_2MoO_3 was used as a model for EXAFS fitting. The bond distance for the first shell of Mo-O in $Li_{1.5}MoO_3$ was determined to be 2.08_8 Å, which is slightly larger in comparison with that in the reference Li_2MoO_3. Also, the curve fitting yields two Mo-Mo bond distances of 2.62_8 and 3.22_8 Å. Though the Debye-Waller factors for each shell are relatively larger, overall fitting could successfully reproduce the FT spectrum of fully charged state, highlighting that the local structure of $Li_{1.5}MoO_3$ resembles that of Li_2MoO_3.

Meanwhile, as the lithium de-intercalation reaction proceeds during the charge (Figure 3B), the merged Mo-O bonds are di-

vided into two FT peaks, which means that most of α-MoO_3 frameworks are restored upon the charge. However, FT amplitude for the spectrum **r** in Figure 3B is quite smaller than that of the pristine MoO_3, showing that the lithium insertion and extraction cause the structural deformation. Furthermore, the shortened Mo-Mo bonds are still discernible around 2.2 Å in the spectrum **r** (non-phase-shift-corrected), which is due to the bond distance of ~2.6 Å. This result reveals that some of the shorten Mo-Mo bonds upon the reduction are not converted into the longer Mo-Mo bonds in α-MoO_3. The present study clearly shows that one of important reasons for poor cyclability of α-MoO_3 in LIB could be such an irreversible phase transformation during the discharge/charge reaction.

Conclusion

The structural change of layered molybdenum oxide during the first cycle was probed by XAS analysis. Electrochemical discharge/charge reaction between Li and MoO_3 led to the noticeable rearrangement of molybdenum and oxygen atoms, which might cause the capacity fading upon the successive cycling. We are under progress in developing new hybrid materials to overcome the capacity fading.

Acknowledgments. This work was supported by National Research Foundation of Korea (SRC: 2010-0001487) and WCU program, and partly by Basic Science Research Program through the National Research Foundation of Korea (NRF) funded by the Ministry of Education, Science and Technology (grant number: 2010-0024370). J. H. Kang thanks to the Ministry of Education, Science and Technology for the Brain Korea 21 (BK21) fellowship.

References

1. Deb, S. K. *Sol. Energy Mater. Sol. Cells* **1995**, *39*, 191.
2. Burcham, L. J.; Briand, L. E.; Wachs, I. E. *Langmuir* **2001**, *17*, 6164.
3. Ferroni, M.; Guidi, V.; Martinelli, G.; Nelli, P.; Sacerdoti, M.; Sberveglieri, G. *Thin Solid Films* **1997**, *307*, 148.
4. Wang, J. F.; Rose, K. C.; Lieber, C. M. *J. Phys. Chem. B* **1999**, *103*, 8405.
5. Chernova, N. A.; Roppolo, M.; Dillon, A. C.; Whittingham, M. S. *J. Mater. Chem.* **2009**, *19*, 2526.
6. Mai, L.; Hu, B.; Chen, W.; Qi, Y.; Lao, C.; Yang, R.; Dai, Y.; Wang, Z. L. *Adv. Mater.* **2007**, *19*, 3712.
7. Kim, M. G.; Cho, J. *Adv. Funct. Mater.* **2009**, *19*, 1497.
8. Bullard, J. W.; Smith, R. L. *Solid State Ionics* **2003**, *160*, 335.
9. Paek, S. M.; Jung, H.; Park, M.; Lee, J. K.; Choy, J. H. *Chem. Mater.* **2005**, *17*, 3492.
10. Paek, S. M.; Jung, H.; Lee, Y. J.; Park, M.; Hwang, S. J.; Choy, J. H. *Chem. Mater.* **2006**, *18*, 1134.
11. Tsumura, T.; Inagaki, M. *J. Mater. Sci. Technol.* **2000**, *16*, 5.
12. Li, W.; Meitzner, G. D.; Borry, R. W.; Iglesia, E. *J. Catal.* **2000**, *191*, 373.
13. Xie, S.; Chen, K.; Bell, A. T.; Iglesia, E. *J. Phys. Chem. B* **2000**, *104*, 10059.
14. Ressler, T.; Wienold, J.; Jentoft, R. E.; Neisius, T. *J. Catal.* **2002**, *210*, 67.
15. Timpe, O.; Neisius, T.; Find, J.; Mestl, G.; Dieterle, M.; Schlögl, R. *J. Catal.* **2000**, *191*, 75.
16. Ressler, T.; Jentoft, R. E.; Wienold, J.; Günter, M. M.; Timpe, O. *J. Phys. Chem. B* **2000**, *104*, 6360.
17. Hibble, S. J.; Fawcett, I. D. *Inorg. Chem.* **1995**, *34*, 500.